EESTI NSV TEADUSTE AKADEEMIA TOIMETISED. KEEMIA
ИЗВЕСТИЯ АКАДЕМИИ НАУК ЭСТОНСКОЙ ССР. ХИМИЯ
PROCEEDINGS OF THE ACADEMY OF SCIENCES OF THE ESTONIAN SSR. CHEMISTRY

1987, 36, 4

https://doi.org/10.3176/chem.1987.4.03

УДК 543.42

Ü. HALDNA, R. A. COX, R. JUGA, E. RAJAVEE

ESTIMATION OF IONS CONCENTRATION IN AQUEOUS SULFURIC ACID MIXTURES BY RESOLUTION OF RAMAN SPECTRA

(Presented by O. Eisen)

The ionic composition of aqueous sulfuric acid solutions has mostly been studied by Raman spectroscopy [1–3]. The majority of researchers have accepted the respective results obtained by H. Chen and D. E. Irish [1]. The concentration profiles of SO_4^{2-} and HSO_4^- presented in [1] have been used for the calculation of the hydrated proton concentration [4] ($C_{H^+} = C_{HSO_4^-} + 2C_{SO_4^{2-}}$). The last quantity ($C_{H^+}$), in turn, plays an important role in determining weak bases basicity constants by the excess acidity method [4]. It should be noted that H. Chen and D. E. Irish [1] discussed the existence of ion pairs $H_3O^+ \cdot SO_4^{2-}$ and $H_3O^+ \cdot HSO_4^-$, but no attempt was made to estimate their concentrations separately from those of the respective nonionpaired species. In recent years, some evidence has been accumulated showing that in the system $H_2SO_4 - H_2O$ both ions, SO_4^{2-} and HSO_4^-, may exist as free ions and as ion pairs [2, 3, 5, 6, 7]. The structure of the latter has been discussed by several authors [5–7]. In the present paper free ions are denoted as HSO_4AQ, SO_4AQ and ionpaired ones as HSO_4IP, SO_4IP, respectively.

H. Chen and D. E. Irish [1] measured the Raman spectra of aqueous sulfuric acid solutions in the range of 2.52—80.58% H_2SO_4 (w/w). In the paper of R. A. Cox et al. [5] the same was done in a wider range, viz. 4.53—99.48% H_2SO_4 (w/w). The mathematical treatment of these spectra [5] was carried out using factor analysis (FA) techniques. Two FA methods have been applied to these spectra [5]: the principal component analysis (PCA) [8] and a novel approach — the spectral isolation analysis (SIA) [9]. The application of FA methods has led to a conclusion that the Raman spectra studied may be presented as a sum of three spectral components which may most likely be assigned to the following sums of species ($SO_4AQ + HSO_4AQ$), ($SO_4IP + HSO_4IP$) and (H_2SO_4) [5, 6]. The latter is the undissociated sulfuric acid detected in concentrated H_2SO_4 solutions. The individual concentration profiles for the species involved were not obtained by the FA methods applied [5, 6]. Nevertheless, PCA [8] followed by the curve-fitting procedures yielded the number of individual but overlapping bands in the spectra studied [5]. Altogether 18 spectral bands were resolved out and their maximum locations determined [5]. This information has been used in the present study in order to obtain concentration profiles for the species present in aqueous sulfuric acid solutions.

Raman spectra and their resolution into bands

The set of spectra used was the same as in [5, 6]. It consists of 25 Raman spectra covering the range of 4.53—96.71% H_2SO_4 (w/w). The experimental part has been published elsewhere [5]. The intensities of spectra

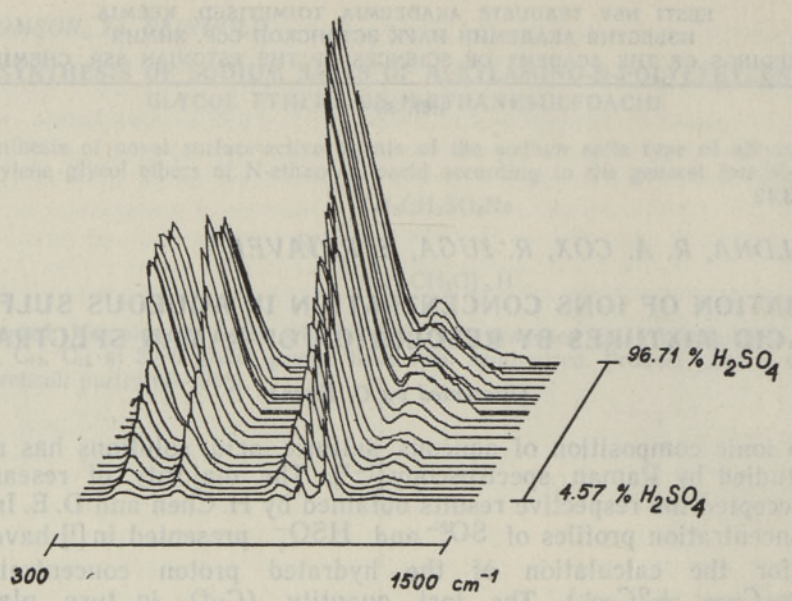

Fig. 1. Standardized Raman spectra of water sulfuric acid mixtures.

were corrected for laser power and signal amplification taking the spectrum of a standard solution (in our case 36.74% H_2SO_4 w/w) before and after each spectrum studied [10]. A factor (H) equal to the mean intensity of the standard solution at 1035 cm^{-1} taken before and after the spectrum studied was calculated. The standardized intensities $I(\nu)$ of the spectra studied were obtained according to the equation [10, 11]

$$I(\nu) = I(\nu)_{obs}/[H \cdot (\nu - \nu_l)^4], \qquad (1)$$

where ν is the wavenumber (cm^{-1}) for the observed intensity $I(\nu)_{obs}$ and ν_l is the wavenumber of the laser line used (20485 cm^{-1} in our case corresponding to the 488 nm line of the argon ion laser). The spectra in analog form were digitalized by hand taking the intensity readings in 10 cm^{-1} steps along the ν-axis. Each recorded band on spectra has been described by 10—15 points (10 cm^{-1} apart from each other). This seems to be sufficient for fixing the bands shape unambiguously. The intensity readings were taken from the baseline constructed by hand using "empty" spectral regions. The intensities were digitalized in the range of 300—1500 cm^{-1} at the same wavenumbers on each spectrum. In this way a spectral data array of 25×120 points was obtained. Fig. 1 shows the standardized spectra. The relative intensities $I(\nu)_{obs}/H$ for the maximum at 1030—1050 cm^{-1} are presented in Table 1. Each spectrum was curve-fitted as a sum of Voigt profiles [12, 13] which are Gaussian—Lorenzian convolutions. Following S. Ikawa and M. Kimura [12] we have used Kielkopf's approximation to the Voigt profile [14] with the additional assumption that the Gaussian part of the profile comes only from the finite slit width, 5 cm^{-1} in our case, i. e. each peak has a Gaussian half-width [5, 13] of 3.0 cm^{-1}. Consequently, each Raman band can be specified by one fixed (β_G) and three adjustable (h, β_L, ν_{max}) parameters (h is the intensity of the band at its maximum ν_{max} and β_G, β_L are half-widths for the Gaussian and Lorenzian part, respectively). The values of ν_{max} from [5] (see Table 2) were used in the iteration procedures as zero approximations. Two bands out of the 18 resolved out in [5] were not used by us (viz. those at 729 cm^{-1} assigned to H_2SO_4, because it is too weak [5, 6], and a band

Table 1

Relative intensity of the maximum at 1030—1050 cm^{-1}

% H_2SO_4	$I_{obs}(\nu)/H$	% H_2SO_4	$I_{obs}(\nu)/H$
4.57	15	65.26	152
8.05	26	67.72	155
11.78	41	69.96	158
15.86	52	75.05	162
21.90	70	80.10	159
23.86	80	84.26	149
31.19	89	87.42	136
36.74	101	89.58	125
44.02	112	90.63	120
50.03	128	92.09	114
54.40	136	94.29	105
58.49	142	96.71	99
59.88	144		

at 590 cm^{-1} assigned to HSO_4IP as it is too close to the band at 595 cm^{-1}). As a result, at 595 cm^{-1} a complex band was resolved out and assigned to SO_4AQ, HSO_4AQ, HSO_4IP [5]. This band as well as those at 433 and 1200 cm^{-1} were further not used to calculate species concentration due to their complex assignments (see Table 2).

Table 2

The spectral bands used in curve-fitting procedures

N	ν_{max}	Assignment	A^*_{max}
1	1361	H_2SO_4	1.8
2	1200	H_2SO_4, HSO_4AQ, HSO_4IP	12.6
3	1147	H_2SO_4	25.6
4	1103	SO_4AQ	0.3
5	1055	HSO_4AQ	8.8
6	1037	HSO_4IP	38.8
7	987	SO_4AQ	12.7
8	935	SO_4IP	3.0
9	918	H_2SO_4	15.2
10	899	HSO_4IP	20.0
11	877	HSO_4AQ	1.3
12	595	SO_4AQ, HSO_4AQ, HSO_4IP	17.2
13	563	H_2SO_4	27.2
14	433	H_2SO_4, SO_4AQ, HSO_4AQ	19.8
15	417	HSO_4IP	4.7
16	395	H_2SO_4	2.4

* Max. values of area in relative but comparable between themselves units.

A program in FORTRAN IV including the standard least-squares curve-fitting subroutine [15] was written which yields optimum values for β_L, ν_{max} and h. Computations were performed on an EC 1052 computer, Institute of Cybernetics, Estonian SSR Academy of Sciences. It should be noted that there exists an "empty" spectral region between 700—800 cm^{-1}. This was used to carry out the curve-fitting procedures for the bands $\nu_{max}>800$ cm^{-1} and $\nu_{max}<700$ cm^{-1} separately. In the range of 1500—800 cm^{-1} 11 bands (the respective maxima at 1361, 1200, 1147, 1103, 1055, 1037, 987, 935, 918, 899, 877 cm^{-1}) and in the range of 700—300 cm^{-1}

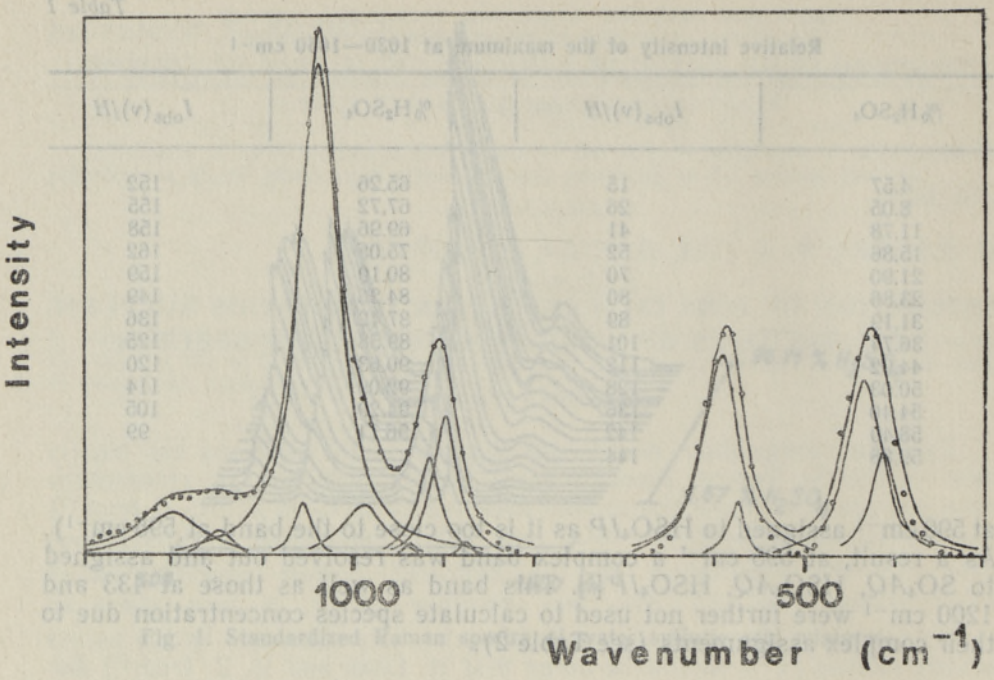

Fig. 2. Experimental spectrum points, resolution bands and calculated spectrum of 75.05% (w/w) aqueous sulfuric acid solution.

Table 3

Areas of peaks (A_i) in the Raman spectra of aqueous sulfuric acid solutions.
Region 1500—800 cm^{-1}

% H_2SO_4	A^*_i for the peak ν_{max} at cm^{-1}											RA**
	1360	1200	1147	1103	1055	1037	987	935	918	899	877	
4.57		0.3			1.1	0.7	1.3	0		0.2	0	36
8.05		0.3			2.5	0.5	2.2	0		1.0	0	31
11.78		0.6			3.8	1.1	2.8	0		1.2	0.5	11
15.86		0.6			4.2	2.1	4.3	0.2		1.8	0.3	11
21.90		1.4			6.1	3.6	6.6	0.5		3.0	0.1	10
23.86		2.1	0		7.2	5.6	7.6	0.8		3.6	0.2	7
31.19		3.2	0.1		7.1	8.4	9.3	1.8		3.6	0.5	6
36.74		2.6	0.2		7.1	10.1	11.0	2.3		4.8	0.1	7
44.02		3.0	0.4		8.8	12.5	11.9	2.6		5.2	0.9	5
50.03		3.0	0.4		7.6	19.4	12.7	2.6	0	6.7	1.2	4
54.40		4.1	0.8		5.3	23.3	12.4	3.0	0.1	6.9	1.3	5
58.49		7.2	0.9		5.6	23.4	11.2	2.2	0.4	7.0	1.2	4
59.88		5.0	1.3		3.6	26.2	11.5	2.2	1.0	7.0	1.0	5
65.26		5.5	1.1		2.0	31.4	9.2	1.9	1.2	7.6	0.8	6
67.72		5.2	1.0	0	2.0	33.0	7.9	1.5	1.7	8.8	0.9	5
69.96		5.2	1.4	0	1.5	36.7	6.5	1.2	2.0	9.0	0.2	5
75.05		6.1	1.3	0.3	1.4	38.2	5.7	1.3	2.5	9.0	0	4
80.10		7.5	1.3	0.2	1.3	38.8	1.6	0.6	3.2	9.4		4
84.26	0	7.8	2.8	0.1	0	38.5	1.2	0	1.9	10.0		4
87.42	0	6.6	5.7	0		38.5	0		3.0	11.5		5
89.58	0.9	9.9	8.6			34.8			7.0	13.0		4
90.63	0.5	12.6	9.4			37.5			8.4	13.5		5
92.09	0.8	7.3	13.7			30.7			7.4	14.5		5
94.29	1.2	7.6	21.4			26.5			9.8	17.0		6
96.71	1.8	10.2	25.6			20.4			15.2	20.0		11

* The units used — see the subscribt to Table 2.
** Ratio RA (Eq. 2).

five peaks (the respective maxima at 595, 563, 433, 417, 395 cm^{-1}) were considered. The curve-fitting procedure was performed several times for each spectrum region using different initial values for β_L, ν_{max} and h every time. The choice of the initial values for β_L and h has a minor influence on band area: the relative scatter in band areas was $<10\%$ of the respective mean value. The areas under the Voigt profiles were obtained by the trapezium method, using 2 cm^{-1} steps. The results of the curve-fitting procedure are presented in Tables 3 and 4 (see Fig. 2). The magnitude of the misfit was estimated by the ratio

$$RA = 100 \cdot A_{a,b}^{-1} \cdot \int_a^b |I(\nu)_{obs} - I(\nu)_{calc}| \, d\nu, \qquad (2)$$

where $A_{a,b}$ is the area under the standardized spectrum observed (Eq. 1) in the region $a \leqslant \nu \leqslant b$ and $I(\nu)_{obs}$, $I(\nu)_{calc}$ are the observed (Eq. 1) and calculated intensity values at the wavenumber ν, respectively. The $I(\nu)_{calc}$ was obtained as a sum of band intensities at the ν considered. The values of RA presented in Tables 3 and 4 demonstrate that the curve-fitting procedure yielded rather good results ($4\% \leqslant RA \leqslant 15\%$).

The ν_{max} values found depend on the stoichiometric acid concentration as shown in Fig. 3. Their values at the respective band area maximum are close to those given in Table 2. The dependence of ν_{max} on the sulfuric acid stoichiometric concentration in the case of bands near 1050 and 980 cm^{-1} has also been found by S. Ikawa [12].

Table 4

Areas of peaks (A_i) in the Raman spectra of aqueous sulfuric acid solutions. Region 300—700 cm^{-1}

% H_2SO_4	A^*_i for the peak ν_{max} at cm^{-1}					RA^{**}
	595	563	433	417	395	
4.57	1.5		1.4			19
8.05	1.9		2.1			15
11.78	2.7		2.7			10
15.86	3.9		3.5			23
21.90	6.6		5.7			18
23.86	7.1		6.7	0		13
31.19	8.0		8.1	0.3		10
36.74	8.2		9.5	0.2		12
44.02	9.4		11.5	0.2		20
50.03	10.6		10.2	2.0		24
54.40	14.5	0	13.1	1.6		11
58.49	17.2	0.2	19.8	1.2		15
59.88	15.0	0.2	19.0	1.5		15
65.26	16.6	0.6	17.0	2.5	0	15
67.72	16.0	0.7	16.9	2.9	0.1	15
69.96	15.6	0.6	12.5	3.2	0.1	25
75.05	14.4	1.8	12.6	4.7	0.4	19
80.10	13.6	3.0	11.8	4.2	0.6	16
84.26	16.1	4.7	10.1	3.4	1.3	6
87.42	13.0	7.0	9.7	2.8	1.4	15
89.58	10.8	13.0	11.0	3.8	1.2	11
90.63	9.8	16.2	10.0	4.6	1.3	11
92.09	10.2	19.8	9.6	3.4	1.5	11
94.29	11.0	22.4	10.8	1.7	1.9	9
96.71	9.7	27.2	10.6	2.5	2.4	10

* The units used — see the subscribt to Table 2.
** Ratio RA (Eq. 2).

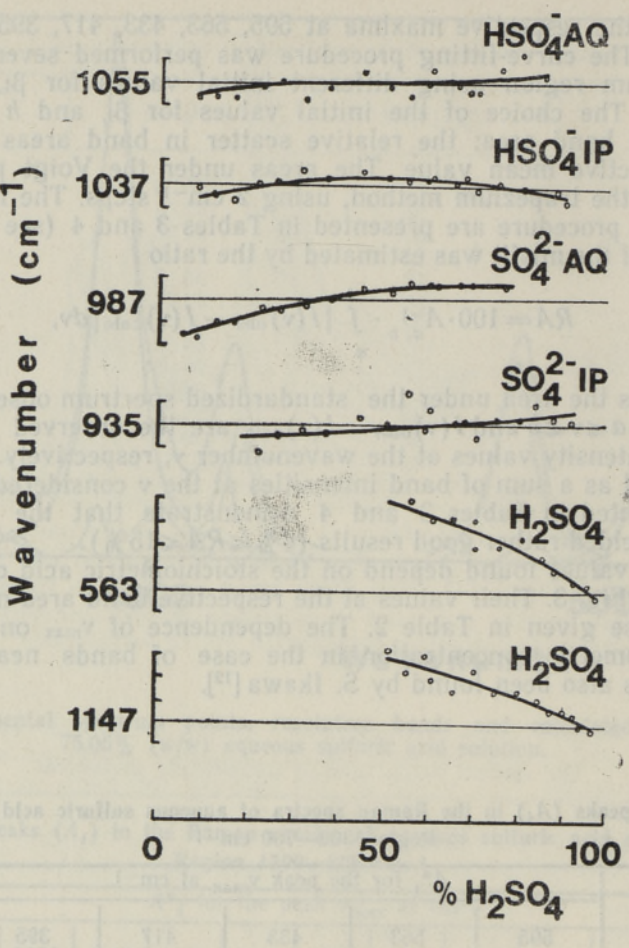

Fig. 3. Dependence of band maximum on stoichiometric acid concentration for the band used. On ordinate axes marks stand for every 5 cm^{-1}.

Species concentration in aqueous sulfuric acid mixtures

Raman band area A is related to the concentration of the species which generates the band through the equation in [10]

$$A = J \cdot C, \tag{3}$$

where J is the specific or molar intensity of the band, and C is the scattering species concentration in moles per liter. The areas of all the bands listed in Table 2 were plotted vs.% H_2SO_4 (except the bands at 1200, 595 and 433 cm^{-1} for the reasons mentioned above; the bands at 1361 and 1103 cm^{-1} were also neglected because of their very small areas). For some bands, mostly rather weak ones at 395, 918 cm^{-1} (both H_2SO_4), 877 cm^{-1} (HSO_4AQ) and 417, 899 cm^{-1} (HSO_4IP) the profiles A vs.% H_2SO_4 (w/w) exhibit quite a remarkable scatter. Therefore these bands were not used for the estimation of species concentrations. After making these exclusions the following bands remained for further treatment: 987 cm^{-1} (SO_4AQ), 1055 cm^{-1} (HSO_4AQ), 935 cm^{-1} (SO_4IP), 1037 cm^{-1} (HSO_4IP), 563 and 1147 cm^{-1} (both for H_2SO_4). The areas of these bands were standardized according to

$$B = A/A_{max}, \tag{4}$$

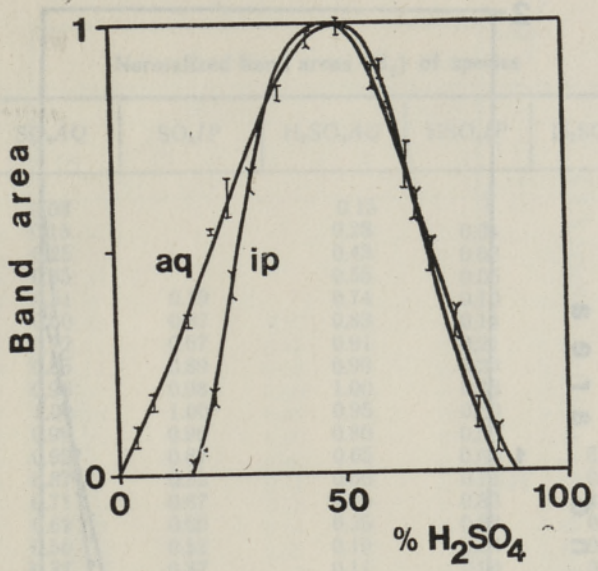

Fig. 4. Normalized areas of the bands specified to SO_4AQ and SO_4IP vs. % (w/w) H_2SO_4. Vertical bars represent uncertainties.

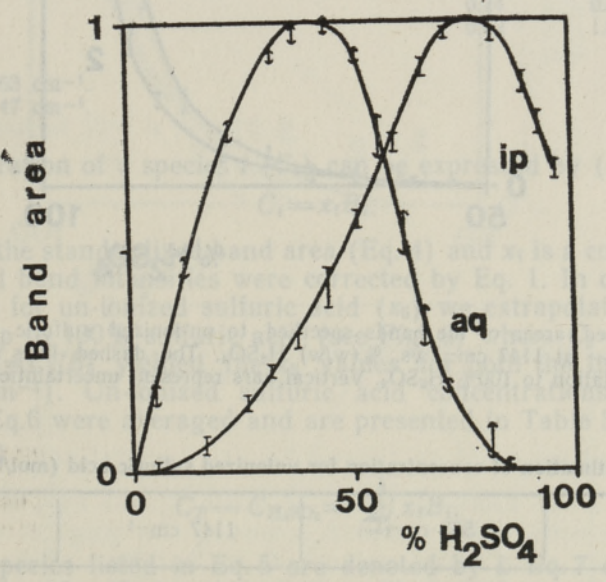

Fig. 5. Normalized areas of the bands specified to HSO_4AQ and HSO_4IP vs. % (w/w) H_2SO_4. Vertical bars represent uncertainties.

where B is the normalized area of the band in the sulfuric acid solution considered, A is the respective area in Table 3 or 4 and A_{max} is the maximum value of A for the band studied (see Table 2). The normalization (Eq. 4) was used in order to give equal weights for all species in regression analysis. The respective examples are shown in Figs 4—6. For a given aqueous sulfuric acid solution with a molar concentration C_T we can write a balance equation

$$C_T = C_{SO_4AQ} + C_{SO_4IP} + C_{HSO_4AQ} + C_{HSO_4IP} + C_{H_2SO_4}. \quad (5)$$

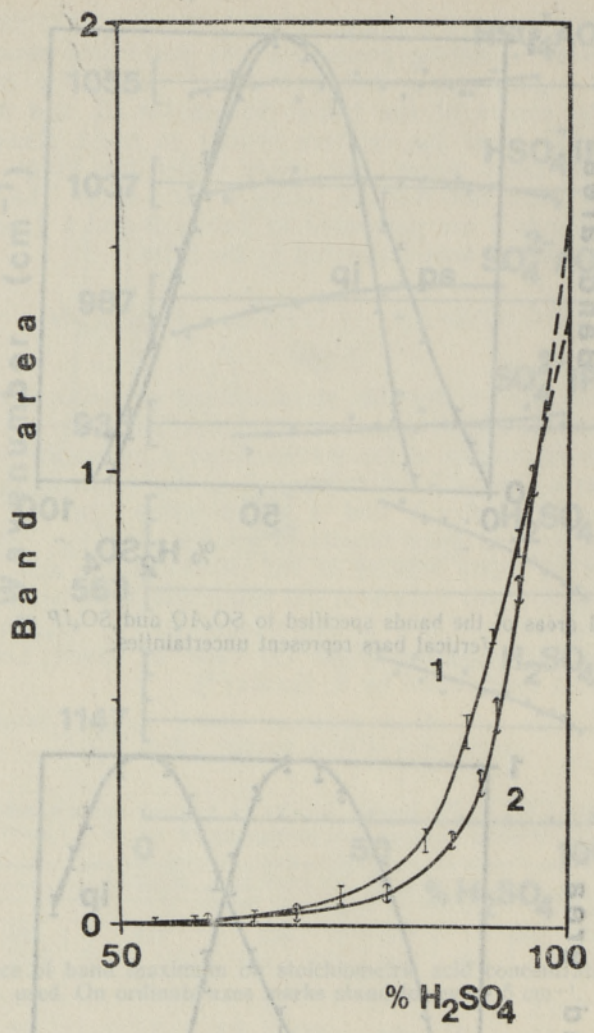

Fig. 6. Normalized areas of the bands specified to un-ionized sulfuric acid. *1* — at 563 cm^{-1} and *2* — at 1147 cm^{-1} vs. % (w/w) H_2SO_4. The dashed lines show the extrapolation to 100% H_2SO_4. Vertical bars represent uncertainties.

Table 5

Estimation of concentration for unionized sulfuric acid (mol/l)

% H_2SO_4	563 cm^{-1}	1147 cm^{-1}	Average
54.40	0	0	0
58.49	0.14	0.12	0.13
59.88	0.14	0.12	0.13
65.26	0.27	0.24	0.26
67.72	0.41	0.24	0.33
69.96	0.41	0.36	0.39
75.05	0.82	0.48	0.65
80.10	1.50	0.84	1.17
84.26	2.60	1.56	2.08
87.42	4.23	2.52	3.38
89.58	7.10	3.60	5.35
90.63	8.05	4.32	6.18
92.09	9.42	5.40	7.41
94.29	11.60	8.15	9.88
96.71	13.65	12.00	12.83

Table 6

Normalized band areas (B_i) of species

% H_2SO_4	SO_4AQ	SO_4IP	H_2SO_4AQ	HSO_4IP	H_2SO_4*	H_2SO_4**
4.57	0.08		0.15			
8.05	0.15		0.28	0.01		
11.78	0.25		0.43	0.03		
15.86	0.35		0.55	0.05		
21.90	0.51	0.19	0.74	0.10		
25.86	0.60	0.37	0.83	0.14		
31.19	0.72	0.67	0.91	0.21		
36.74	0.85	0.89	0.99	0.29		
44.02	0.96	0.98	1.00	0.38		
50.03	1.00	1.00	0.95	0.50		
54.40	0.99	0.96	0.80	0.58		
58.49	0.92	0.87	0.65	0.68	0.01	0.01
59.88	0.87	0.82	0.56	0.71	0.01	0.01
65.26	0.71	0.67	0.35	0.83	0.02	0.02
67.72	0.62	0.59	0.25	0.88	0.03	0.02
69.96	0.56	0.52	0.19	0.94	0.03	0.03
75.05	0.37	0.37	0.11	0.99	0.06	0.04
80.10	0.10	0.22	0.04	1.00	0.11	0.07
84.26				0.97	0.19	0.13
87.42				0.92	0.31	0.21
89.58				0.85	0.52	0.30
90.63				0.83	0.59	0.36
92.09				0.79	0.69	0.45
94.29				0.74	0.85	0.68
96.71				0.62	1.00	1.00

* Peak at 563 cm^{-1}.
** Peak at 1147 cm^{-1}.

The concentration of a species i (C_i) can be expressed by (see also Eq. 3)

$$C_i = x_i B_i, \tag{6}$$

where B_i is the standardized band area (Eq. 4) and x_i is a constant because the observed band intensities were corrected by Eq. 1. In order to obtain the x_i value for un-ionized sulfuric acid (x_5) we extrapolated the plot B_5 vs.% acid up to 100% sulfuric acid (see Fig. 6) where $C_5 = 18{,}61$ mole/L. The ratio $x_5 = C_5/B_5$ yielded the x_5 values for both the lines used (563 and 1147 cm^{-1}). Un-ionized sulfuric acid concentrations ($C_{H_2SO_4}$) calculated by Eq.6 were averaged and are presented in Table 5. This enables us to obtain

$$C_T - C_{H_2SO_4} = \sum_{i=1}^{4} x_i B_i, \tag{7}$$

where the species listed in Eq. 5 are denoted by i. Eq. 7 can be written for each of the 25 sulfuric acid solutions. This yields a set of 25 equations with 4 unknown coefficients ($x_1, \ldots, x_4$). Using the B_i values from Table 6 the following regression coefficients were obtained: SO_4AQ, $x_1 = -1.75 \pm 4.44$, SO_4IP, $x_2 = -0.29 \pm 3.23$, HSO_4AQ, $x_3 = 3.07 \pm 2.23$ and HSO_4IP, $x_4 = 12.60 \pm 0.66$ (the respective standard deviations at $f = 20$ are also presented). The negative values of x_1 and x_2 are meaningless and x_3 is rather uncertain. This result is not unexpected because the scales B_1, B_2 and B_3 are strongly correlated among themselves: $R_{1,2} = 0.946$, $R_{1,3} = 0.744$ and $R_{2,3} = 0.595$. The $R_{1,2}$ value implies that there is no possibility of differentiating SO_4AQ and SO_4IP concentrations. In this situation the use of the equation

$$C_T - C_{H_2SO_4} - C_{SO_4^{2-}} = x_3 B_3 + x_4 B_4 \tag{8}$$

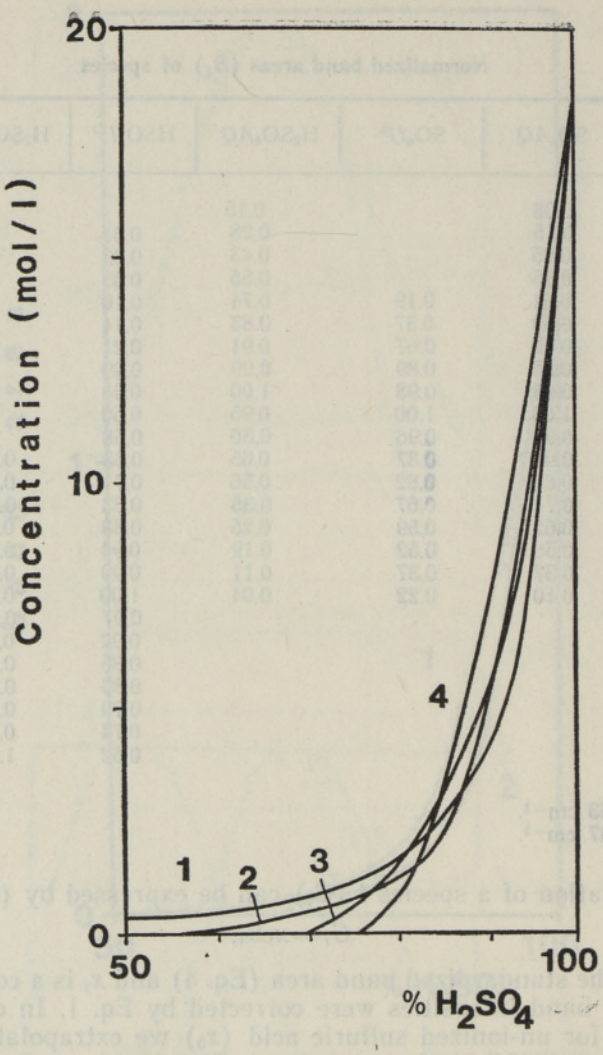

Fig. 7. Comparison of un-ionized sulfuric acid concentrations vs. % (w/w) H_2SO_4 estimated by different authors. *1* — from [5], *2* — present study, *3* — from [3] and *4* — from [2].

is probably best we could do (where $C_{SO_4^{2-}}$ is the total SO_4^{2-} concentration estimated by N. B. Librovich [2] or H. Chen [1]; see Fig. 8). Eq. 8 was applied to the data of 17 solutions (covering the range of 4.57—75.05% H_2SO_4). Using the $C_{SO_4^{2-}}$ values of N. B. Librovich [2] we obtained $x_3 = 0.86 \pm 0.35$ and $x_4 = 11.06 \pm 0.41$. The respective results with H. Chen's data [1] were $x_3 = 0.71 \pm 0.39$ and $x_4 = 10.07 \pm 0.46$. Assuming that the $C_{SO_4^{2-}}$ values found by N. B. Librovich [2] and H. Chen [1] are probably the sum $C_{SO_4AQ} + C_{SO_4IP}$ we used the equation

$$C_{SO_4^{2-}} = x_1 B_1 + x_2 B_2 \qquad (9)$$

to obtain x_1 and x_2. If $C_{SO_4^{2-}}$ was taken from [2], $x_1 = 0.92 \pm 0.18$, $x_2 = 0.12 \pm 0.19$ and respectively, the data of H. Chen [1] yielded $x_1 = 1.02 \pm 0.94$ and $x_2 = 0.90 \pm 1.00$.

The concentration profiles of SO_4AQ, SO_4IP, HSO_4AQ, HSO_4IP and H_2SO_4 estimated in this paper (Eq. 6) are presented in Table 7. A comparison of the data from Table 7 with the respective earlier ones (see

Table 7

Concentrations of species (mol/l)

C_T	SO_4AQ		SO_4IP		HSO_4AQ		HSO_4IP		H_2SO_4
	[2]	[1]	[2]	[1]	2	1	2	1	
0.478	0.07	0.08			0.13	0.11			
0.862	0.14	0.15			0.24	0.20	0.11	0.10	
1.291	0.23	0.25			0.37	0.30	0.33	0.30	
1.788	0.32	0.36			0.47	0.39	0.55	0.50	
2.571	0.47	0.52	0.02	0.17	0.64	0.52	1.11	1.01	
3.116	0.55	0.61	0.05	0.33	0.72	0.59	1.55	1.41	
3.896	0.66	0.73	0.08	0.60	0.78	0.64	2.32	2.12	
4.761	0.78	0.87	0.11	0.80	0.85	0.70	3.21	2.92	
5.991	0.88	0.98	0.12	0.88	0.86	0.71	4.20	3.83	
7.098	0.92	1.02	0.12	0.90	0.82	0.67	5.53	5.04	
7.958	0.91	1.01	0.12	0.86	0.69	0.57	6.41	5.84	
8.813	0.84	0.94	0.11	0.78	0.56	0.46	7.52	6.85	0.13
9.114	0.80	0.89	0.10	0.73	0.48	0.40	7.85	7.15	0.13
10.32	0.65	0.72	0.08	0.60	0.30	0.25	9.18	8.36	0.26
10.91	0.57	0.63	0.07	0.53	0.22	0.18	9.73	8.86	0.33
11.45	0.51	0.57	0.06	0.47	0.16	0.13	10.40	9.47	0.39
12.74	0.34	0.38	0.05	0.33	0.09	0.08	10.95	9.97	0.65
14.07	0.09	0.10	0.03	0.20			11.06	10.07	1.17
15.17							10.70	9.77	2.08
15.93							10.20	9.26	3.38
16.50							9.40	8.56	5.35
16.75							9.15	8.36	6.18
17.08							8.74	7.96	7.41
17.56							8.20	7.45	9.88
18.05							6.85	6.21	12.83

1 — concentration of SO_4^{2-} is from [1].

2 — concentration of SO_4^{2-} is from [2].

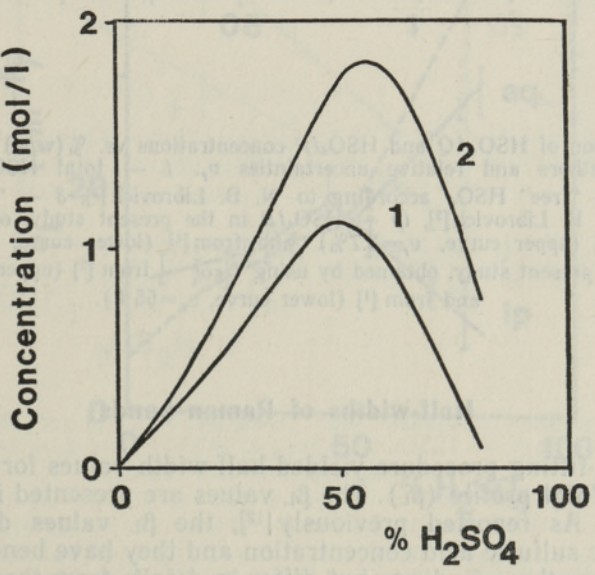

Fig. 8. Comparison of SO_4^{2-} concentrations vs. % (w/w) H_2SO_4 estimated by different authors. *1* — from [2], *2* — from [1].

Figs 7 and 9) leads to the following conclusions. First, the mean concentration profile for un-ionized sulfuric acid (see Fig. 7) agrees rather well with the earlier estimates [2, 3, 5]. Second, the results of H. Chen and D. E. Irish [1] are purely based on the relative integrated intensity of the band at 981 cm^{-1} assigned to the sulfate ion. Their $C_{HSO_4^-} = C_T - C_{SO_4^{2-}}$. Therefore, disagreement with these concentration profiles [1] is not surprising. Third, the study of N. B. Librovich [2] is based on the unresolved bands and the concentration of HSO_4IP has been calculated as a difference $C_T - (C_{H_2SO_4} + C_{HSO_4^-} + C_{SO_4^{2-}})$. This results in large disagreement between species concentration profiles of his paper [2] and those of the present study (see Fig. 9).

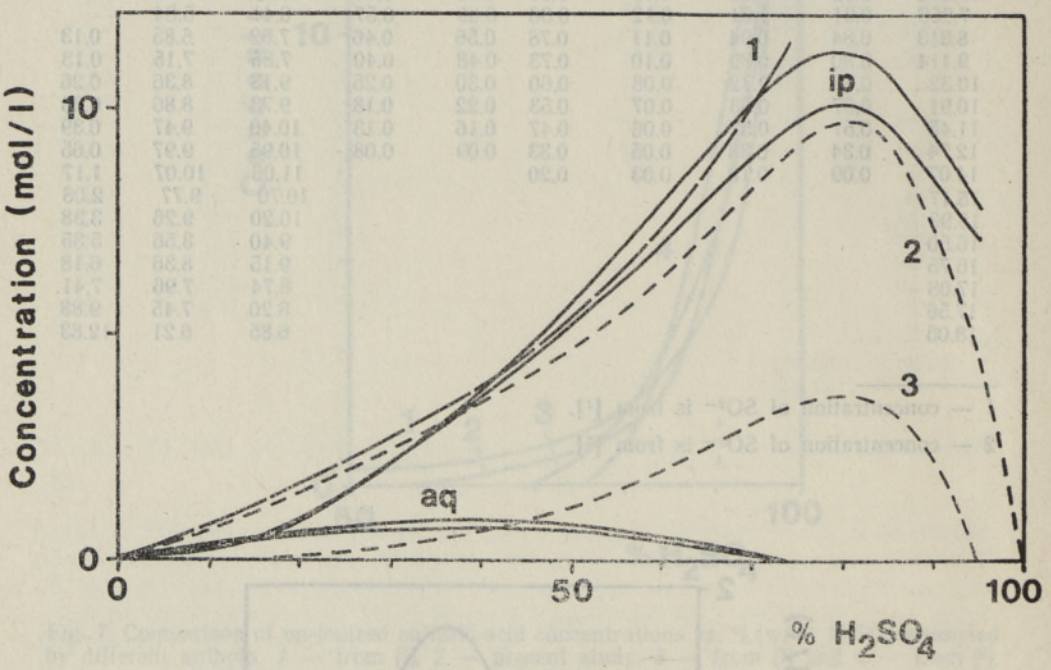

Fig. 9. Comparison of HSO_4AQ and HSO_4IP concentrations vs. % (w/w) H_2SO_4 estimated by different authors and relative uncertainties v_r. *1* — total HSO_4, estimated by H. Chen [1], *2* — "free" HSO_4 according to N. B. Librovich [2], *3* — "ionpaired" HSO_4 according to N. B. Librovich [2], *ip* — HSO_4IP in the present study, obtained by using $C_{SO_4^{2-}}$ from [2] (upper curve, v_r=3.7%) and from [1] (lower curve, v_r=4.6%), *aq* — HSO_4AQ in the present study, obtained by using $C_{SO_4^{2-}}$ from [2] (upper curve, v_r=40%) and from [1] (lower curve, v_r=55%).

Half-widths of Raman bands

The curve-fitting procedure yielded half-width values for the Lorenzian part of the Voigt profile (β_L). The β_L values are presented in Table 8 and Figs 10—12. As reported previously [12], the β_L values depend on the stoichiometric sulfuric acid concentration and they have bends. In general, our data assure these findings but differ in details from those of S. Ikawa and M. Kimura [12]; see Figs 10 and 11. It should be pointed out that in two cases (for bands at 935 and 1055 cm^{-1}) our β_L values have maxima

Table 8

Half-widths of Lorenzian component in Raman spectra (cm^{-1})

% H_2SO_4	SO_4AQ	SO_4IP	HSO_4AQ	HSO_4IP	H_2SO_4
4.57	13.0		8.6	12.0	
8.05	12.5		9.2	13.2	
11.78	11.4		10.3	15.2	
15.86	12.0		10.2	16.0	
21.90	13.6	13.0	10.4	14.0	
25.86	13.0	16.1	10.6	14.8	
31.19	14.6	15.2	11.8	19.6	
36.74	14.8	17.0	11.4	19.4	
44.02	15.5	17.1	12.4	18.5	
50.02	17.5	21.0	12.4	21.6	
54.40	19.2	19.5	12.2	20.4	
58.49	18.7	16.0	11.8	20.4	4.0
59.88	20.4	13.2	10.5	20.6	4.6
65.26	22.6	11.0	10.0	21.4	5.2
67.72	21.8	12.0	9.8	22.3	8.0
69.96	24.5	11.4	11.0	24.1	7.8
75.05	27.0	12.0	10.9	23.6	10.0
80.10	27.4	7.1	10.2	23.9	10.3
84.26			9.8	24.0	12.8
87.42				26.0	15.6
89.58				27.2	18.5
90.63				26.3	19.5
92.09				27.4	19.4
94.29				27.4	19.3
96.71				24.8	18.4

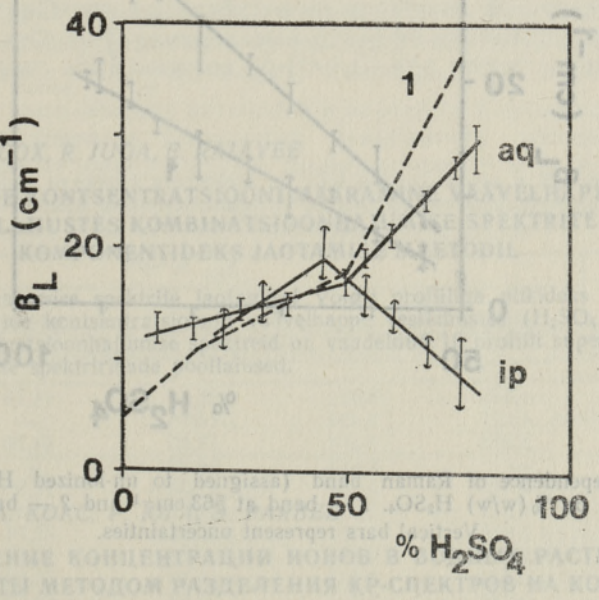

Fig. 10. The dependence of Raman band (assigned to sulfate ions) Lorenzian half-width (β_L) on % (w/w) H_2SO_4. *1* — from [12], *aq* — SO_4AQ band at 987 cm^{-1} and *ip* — SO_4IP band at 935 cm^{-1}. Vertical bars represent uncertainties.

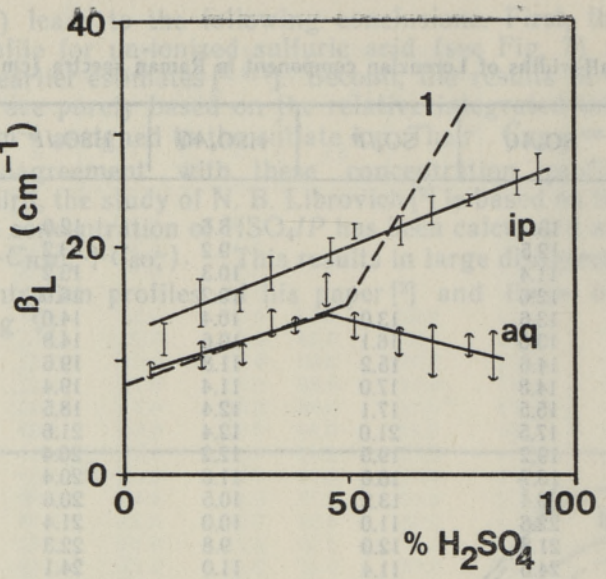

Fig. 11. The dependence of Raman band (assigned to bisulfate ions) Lorenzian half-width (β_L) on % (w/w) H_2SO_4. *1* — from [12], *aq* — HSO_4AQ band at 1055 cm^{-1} and *ip* — HSO_4IP band at 1037 cm^{-1}. Vertical bars represent uncertainties.

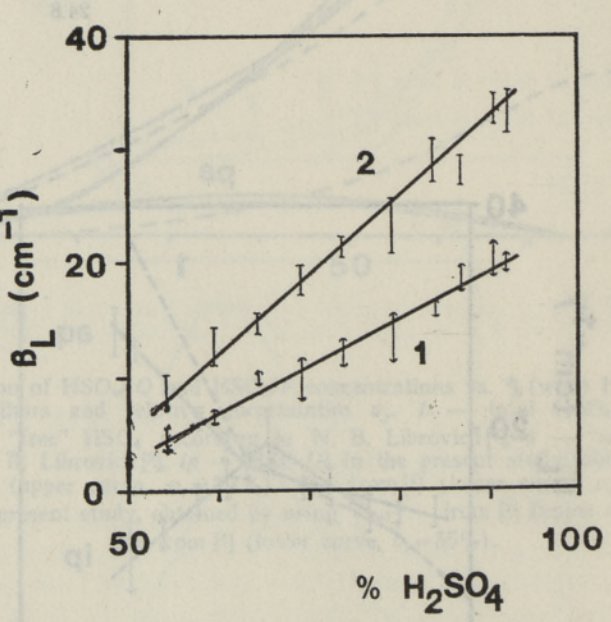

Fig. 12. The dependence of Raman band (assigned to un-ionized H_2SO_4) Lorenzian half-width (β_L) on % (w/w) H_2SO_4. *1* — band at 563 cm^{-1} and *2* — band at 1147 cm^{-1}. Vertical bars represent uncertainties.

at 45% H_2SO_4 and bend down with increasing stoichiometric concentration. This indicates that the mean spectroscopic lifetimes of respective species (SO_4IP and HSO_4AQ) pass through a minimum and increase if the stoichiometric acid concentration exceeds 45%.

REFERENCES

1. *Chen, H., Irish, D. E.* A Raman spectral study of bisulfate sulfate system. II. Constitution, equilibria, and ultrafast proton transfer in sulfuric acid. — J. Phys. Chem., 1971, **75**, 2072.
2. *Либрович Н. Б., Майоров В. Д.* Ионно-молекулярный состав водных растворов серной кислоты при 25°. — Изв. АН СССР. Сер. хим., 1977, **51**, 684.
3. *Зараханн Н. Г., Маркин В. С., Залков Г. Е.* Гомогенные каталитические активные растворы. XII. Равновесный состав кислоты при 25°. — Изв. АН СССР. Сер. хим., 1979, **53**, 2294.
4. *Cox, R. A., Yates, K.* Excess acidities. A generalized method for the determination of basicities in aqueous acid mixtures. — J. Amer. Chem. Soc., 1978, **100**, 3861.
5. *Cox, R. A., Haldna, Ü. L., Idler, K. L., Yates, K.* Resolution of Raman spectra of aqueous sulfuric acid mixtures using principal factor analysis. — Can. J. Chem., 1981, **59**, 2591.
6. *Malinovski, E. R., Cox, R. A., Haldna, Ü. L.* Factor analysis for isolation of the Raman spectra of aqueous sulfuric acid components. — Anal. Chem., 1984, **56**, 778.
7. *Irish, D. E., Chen, H.* Equilibria and proton transfer in the bisulfate-sulfate system. — J. Phys. Chem., 1970, **74**, 3796.
8. *Simonds, J. L.* Application of characteristic vector analysis to photographic optical response data. — J. Opt. Soc. Amer., 1963, **53**, 968.
9. *Malinowski, E. R.* Obtaining the key set of typical vectors by factor analysis and subsequent isolation of component spectra. — Anal Chim. Acta, 1982, **134**, 129.
10. *Irish, D. E., Chen, H.* The application of Raman spectroscopy to chemical analysis. — Appl. Spectrosc., 1971, **25**, 1.
11. *Long, D. A.* Raman Spectroscopy. New York, 1977, 56.
12. *Ikawa, S., Kimura, M.* The study of the Raman band shape of sulfuric acid and proton transfer. — Bull. Chem. Soc. Jap., 1976, **49**, 2051.
13. *Seshadri, J. S., Jones, R. N.* The shapes and intensities of infrared absorption bands. — Spectrochim. Acta, 1963, **19**, 1013.
14. *Kielkopf, J. F.* New approximation to the Voigt function with application to spectral line profile analysis. — J. Opt. Soc. Amer., 1973, **63**, 987.
15. *Bevington, P. R.* Data Reduction and Error Analysis for the Physical Sciences. New York, 1969, 272.

Academy of Sciences of the Estonian SSR,
Institute of Chemistry

Received
Dec. 30, 1986

University of Toronto

Ü. HALDNA, R. A. COX, R. JUGA, E. RAJAVEE

IOONIDE KONTSENTRATSIOONI MÄÄRAMINE VÄÄVELHAPPE VESILAHUSTES KOMBINATSIOONHAJUMISE SPEKTRITE KOMPONENTIDEKS JAOTAMISE MEETODIL

Kombinatsioonhajumise spektrite jaotamisel Voigti profiiliga piikideks on määratud ioonide ja ioonpaaride kontsentratsioonid väävelhappe vesilahustes (H_2SO_4 massi % on 4,57—96,71). Kombinatsioonhajumise spektreid on vaadeldud 16 profiili superpositsioonina ja määratud osakeste spektriribade poollaiused.

Ю. ХАЛДНА, Р. А. КОКС, Р. ЮГА, Э. РАЯВЕЕ

ОПРЕДЕЛЕНИЕ КОНЦЕНТРАЦИИ ИОНОВ В ВОДНЫХ РАСТВОРАХ СЕРНОЙ КИСЛОТЫ МЕТОДОМ РАЗДЕЛЕНИЯ КР-СПЕКТРОВ НА КОМПОНЕНТЫ

Путем разделения КР-спектров на профили Фойгта определены концентрации ионов и ионных пар в водных растворах серной кислоты в интервале 4,57—96,71% мас. H_2SO_4. КР-спектры рассмотрены в суперпозиции 16 отдельных полос. Для частиц определены значения ширин полос на полувысоте.